

Constraints on ultra-slow-roll inflation with the NANOGrav 15-Year Dataset

Bo Mu^{1,2,*}, Jing Liu^{1,2,†}, Gong Cheng^{1,2,‡} and Zong-Kuan Guo^{3,4,5§}

¹*International Centre for Theoretical Physics Asia-Pacific,
University of Chinese Academy of Sciences, 100190 Beijing, China*

²*Taiji Laboratory for Gravitational Wave Universe,
University of Chinese Academy of Sciences, 100049 Beijing, China*

³*CAS Key Laboratory of Theoretical Physics, Institute of Theoretical Physics,
Chinese Academy of Sciences, P.O. Box 2735, Beijing 100190, China*

⁴*School of Physical Sciences, University of Chinese Academy of Sciences,
No.19A Yuquan Road, Beijing 100049, China and*

⁵*School of Fundamental Physics and Mathematical Sciences, Hangzhou Institute for Advanced Study,
University of Chinese Academy of Sciences, Hangzhou 310024, China*

Ultra-slow-roll (USR) inflation predicts an exponential amplification of scalar perturbations at small scales, which leads to a stochastic gravitational wave background (SGWB) through the coupling of the scalar and tensor modes at the second-order expansion of the Einstein equation. In this work, we search for such a scalar-induced SGWB from the NANOGrav 15-year (NG15) dataset, and find that the SGWB from USR inflation could explain the observed data. We place constraints on the amplitude of the scalar power spectrum to $P_{\text{Rp}} > 10^{-1.80}$ at 95% confidence level (C.L.) at the scale of $k \sim 20 \text{ pc}^{-1}$. We find that $\log_{10} P_{\text{Rp}}$ degenerates with the peak scale $\log_{10} k_{\text{p}}$. We also obtain the parameter space allowed by the data in the USR inflationary scenario, where the e -folding numbers of the duration of the USR phase has a lower limit $\Delta N > 2.80$ (95% C.L.) when the USR phase ends at $N \approx 20$. Since the priors for the model parameters are uncertain, we do not calculate the Bayes factors. Instead, to quantify the goodness of fit, we calculate the maximum values of the log-likelihood for USR inflation, bubble collision of the cosmological phase transition, and inspiraling supermassive black hole binaries (SMBHBs), respectively. Our results imply that the SGWB from USR inflation can fit the data better than the one from SMBHBs.

Introduction. The direct detection of gravitational waves (GWs), which are the ripples of spacetime predicted by general relativity, opens a new era of the exploration of the early Universe [1–3]. The monumental discovery was the detection of the merger of two black holes by LIGO which provides a new way to observe the Universe, complementing traditional electromagnetic observations. SGWBs are formed from the superpositions of many unresolved GW sources, of both astrophysical and cosmological origins, which can be detected by searching for correlated signals between multiple detectors. Searching for such SGWBs has been the main scientific goal of multiband GW observers including LIGO-Virgo-KAGRA, LISA, Taiji, TianQin, and pulsar timing array (PTA) experiments.

Recently, the PTA experiments, including CPTA [4], NANOGrav [5], PPTA [6] and EPTA [7], collectively announced the first positive evidence of SGWBs at the nanohertz frequency band ($\sim 1 - 100 \text{ nHz}$). Based on the evolution of the Universe, it is predicted that a cosmic population of supermassive black hole binaries generates a SGWB at the nanohertz frequency band, which is treated as the fiducial model in the analysis of NANOGrav-15 dataset [8]. However, the detected GW power spectrum deviates from that given by the expected values of each parameter [9]. Actually there are also other potential GW sources at this frequency band, such as cosmological phase transitions [10–12], cosmic topological defects [13–17], and primordial scalar perturbations [18–

21], which generate SGWBs in the early Universe. It is found that some of these cosmological sources can explain the NANOGrav data more properly [22]. In their work, three parameterization templates for the power spectrum of scalar perturbations, which sources the energy spectrum of scalar-induced gravitational waves (SIGWs), have been considered.

In this paper, we fit the NG15 data with the SGWB from ultra-slow-roll (USR) inflation, which is a physical well-motivated SIGW model. In the USR inflationary scenario, where the slow-roll approximation is not adhered to, the superhorizon evolution of scalar perturbations can lead to exponential amplification as calculated in various studies [23–25]. The USR regime arises from the non-attractor evolution of the inflaton field, which can be manifested through modified gravity theories [26–28], string theory approaches [29–31], and supergravity models [32–34]. Additionally, minor fluctuations in the inflationary potential – encompassing features like bumps [35, 36], dips [35, 37], inflection points [38–40], and steps [41–44] – might also be considered as possible triggers for the USR regime. A myriad of references [45–60] suggest that enhanced curvature perturbations might pave the way for the emergence of primordial black holes housing dark matter, rendering USR inflation a subject of keen interest. Based on CMB observations, the amplitude of the primordial scalar power spectrum is firmly constrained to be around 2.10×10^{-9} [61]. Nonetheless, at smaller scales, these constraints might be more flexi-

ble [62, 63]. The USR domain can also yield significant e -folding numbers, crucial parameters for addressing horizon, flatness, and monopole issues [64]. The core objective of our research is to discern the constraints that the NG15 dataset might impose on the inflationary potential of the USR regime as well as on the power spectrum of scalar perturbations. For convenience, $c = 8\pi G = 1$ is set throughout this paper.

PTA Data. We use the NG15 dataset, which comprises the pulse time of arrival (ToAs) for 68 millisecond pulsars. With a timing baseline of 3 years, 67 of these pulsars remain viable for processing. NANOGrav fits these ToAs to a timing model that encapsulates the sky location, proper motion, parallax, pulsar spin period, and spin period derivative for each pulsar [8].

We use the Python package `PTArcade` [65] to perform the Bayesian analysis, which integrates new physics into the PTA data analysis package `ENTERPRISE` [66]. The new physics are characterized by the GW spectrum, denoted as Ω_{GW} . Except for Ω_{GW} , we set other parameters by default, such as the ephemeris model included in the timing model.

Then, we will briefly introduce the likelihood function used in this work. The pulsar's timing residuals $\delta\mathbf{t}$ can be modeled as

$$\delta\mathbf{t} = \mathbf{n} + \mathbf{M}\boldsymbol{\epsilon} + \mathbf{F}\mathbf{a}, \quad (1)$$

where \mathbf{n} describes the white noise, $\mathbf{M}\boldsymbol{\epsilon}$ represents the errors associated with the best-fitting timing-ephemeris parameters [67]. The term $\mathbf{F}\mathbf{a}$ characterizes the red noise, which is presumed to be a combination of pulsar-intrinsic red noise and SGWB signals. The matrix \mathbf{F} is the Fourier basis matrix, constructed from sine-cosine pairs based on the ToAs with frequencies defined as $f_i = i/T_{\text{obs}}$, where $T_{\text{obs}} = 16.03\text{yr}$ is the timing baseline for the entire NG15 dataset. For the Fourier amplitudes, \mathbf{a} follows a zero-mean normal distribution with a covariance matrix $\langle\mathbf{a}\mathbf{a}^T\rangle = \boldsymbol{\phi}$, which is given by

$$\langle\phi\rangle_{(ak)(bj)} = \delta_{ij}(\delta_{ab}\varphi_{a,i} + \Gamma_{ab}\Phi_i). \quad (2)$$

The first term characterizes the pulsar-intrinsic red noise, which is defined as a power-law function in this work, with the coefficients $\varphi_{a,i}$ modeled as

$$\varphi_{a,i}(f) = \frac{A_a^2}{12\pi^2} \frac{1}{T_{\text{obs}}} \left(\frac{f}{1\text{yr}^{-1}}\right)^{-\gamma_a} \text{yr}^3, \quad (3)$$

and the priors of A_a, γ_a are shown in Table I. In the second term, Γ_{ab} is defined based on the Hellings & Downs ("HD") correlation [68]. Φ_i is related to the SGWB spectrum as

$$\Omega_{\text{GW}}(f) \equiv \frac{1}{\rho_c} \frac{d\rho_{\text{GW}}(f)}{d\ln(f)} = \frac{8\pi^4 f^5}{H_0^2} \frac{\Phi(f)}{\Delta f}. \quad (4)$$

Here $H_0 = h \times 100 \text{ km s}^{-1} \text{ Mpc}^{-1}$ is the Hubble constant, $\Delta f = 1/T_{\text{obs}}$, and $\Phi(f)$ is defined as $\Phi_i = \Phi(i/T_{\text{obs}})$.

Upon marginalizing over $\mathbf{a}, \boldsymbol{\epsilon}$, we obtain a likelihood that only depends on the parameters that affecting $\langle\mathbf{a}\mathbf{a}^T\rangle$. The likelihood is expressed as

$$p(\delta\mathbf{t}|\boldsymbol{\phi}) = \frac{\exp\left(-\frac{1}{2}\delta\mathbf{t}^T \mathbf{C}^{-1} \delta\mathbf{t}\right)}{\sqrt{\det(2\pi\mathbf{C})}}, \quad (5)$$

where $\mathbf{C} = \mathbf{N} + \mathbf{T}\mathbf{B}\mathbf{T}^T$, \mathbf{N} is the covariance matrix of \mathbf{n} , $\mathbf{T} = [\mathbf{M}, \mathbf{F}]$, and $\mathbf{B} = \text{diag}(\infty, \boldsymbol{\phi})$. Here, ∞ represents a diagonal matrix filled with infinities, implying that the priors for parameters in $\boldsymbol{\epsilon}$ are assumed to be flat.

SGWB from USR inflation. Under the slow-roll approximation, the Fourier modes of curvature perturbations, R_k , remain constant at superhorizon scales. Refs. [23–25] find that during the USR regime at superhorizon scales, the time derivative of R_k , denoted as \dot{R}_k , undergoes exponential amplification. Consequently, the primordial scalar power spectrum P_R derived from R_k reaches its peak at the beginning of the USR inflation. Ref. [23] suggests that P_R behaves as $P_R \propto k^4$ on the infrared side of the peak, and $P_R \propto k^\beta$ on the ultraviolet side, with β depending on the inflationary potential. Given that the USR inflation ends at $\phi = \phi_e$, the Taylor expansion of the inflationary potential around ϕ_e is

$$V(\phi) = b_0 + b_1(\phi - \phi_e) + b_2(\phi - \phi_e)^2 + \dots \quad (6)$$

With more detailed assumptions and further calculation [23], one can obtain

$$\beta = 3 - \sqrt{9 - 24b_2/b_0}, \quad (7)$$

which can be treated as a constant as long as ϕ is in the vicinity of ϕ_e . $\dot{\phi}$ exponentially decreases during the USR regime, after which ϕ stays close to ϕ_e for a long period during inflation so that the expansion (6) remains valid.

Instead of numerically calculating the exact form of $P_R(k)$, we parameterize the power spectrum of curvature perturbations in USR inflationary models as

$$P_R(k) = P_{R\text{p}} \frac{(\alpha + \beta)^\gamma}{\left[\beta(k/k_{\text{p}})^{-\alpha/\gamma} + \alpha(k/k_{\text{p}})^{\beta/\gamma}\right]^\gamma}, \quad (8)$$

where $P_R(k)$ reaches its peak value $P_{R\text{p}}$ at $k = k_{\text{p}}$, and we set $\alpha = 4$ following the relation $P_R \propto k^4$. The parameter γ characterizes the smoothness of $P_R(k)$ around the peak. Since γ does not significantly affect the results, we adopt a representative value of $\gamma = 2.6$ in this work. Then, the remaining free parameters are $P_{R\text{p}}, k_{\text{p}}$, and β .

Given the form of $P_R(k)$, we are able to numerically calculate the GW energy spectrum $\bar{\Omega}_{\text{GW}}(k)$ in the radiation-dominated era, following the integration method in Refs. [69, 70]

$$\begin{aligned} \bar{\Omega}_{\text{GW}}(k) = & \int_0^\infty dv \int_{|1-v|}^{1+v} \left(\frac{4v^2 - (1+v^2 - u^2)^2}{4uv} \right)^2 \\ & \times \text{IRD}_{sq}(u, v) P_R(ku) P_R(kv), \end{aligned} \quad (9)$$

in which $IRD_{sq}(u, v)$ is a function of u, v ,

$$IRD_{sq}(u, v) = \frac{1}{2} \left(\frac{3(u^2 + v^2 - 3)^2}{4u^3v^3} \right)^2 \times \left[\left(-4uv + (u^2 + v^2 - 3) \ln \left| \frac{3 - (u+v)^2}{3 - (u-v)^2} \right| \right)^2 + \pi^2 (u^2 + v^2 - 3)^2 \Theta(u + v - \sqrt{3}) \right], \quad (10)$$

where $\Theta(x)$ is the heaviside step function.

Furthermore, using the relationship $f \approx 0.03 \text{ Hz} \frac{k}{2 \times 10^7 \text{ pc}^{-1}}$, we could express $\bar{\Omega}_{\text{GW}}(k)$ in terms of the corresponding frequency f . Repeatedly calculating this integration for every step would be computationally expensive. As the integral is simply proportional to P_{Rp}^2 , we extract P_{Rp}^2 from the integral. So now the integral only depends on the other two parameters β and f_p . Then we compute the integration in the β - f_p grid. So for any given values of β and f_p , we can infer the integral by using 2-D interpolation.

The energy spectrum of SGWB at present $\Omega_{\text{GW}}(f)$ is related to $\bar{\Omega}_{\text{GW}}(f)$ as

$$\Omega_{\text{GW}}(f) = \Omega_r \left(\frac{g_*(f)}{g_*^0} \right) \left(\frac{g_{*,s}^0}{g_{*,s}(f)} \right)^{4/3} \bar{\Omega}_{\text{GW}}(f), \quad (11)$$

where Ω_r is the present energy density fraction of radiation, g_* and $g_{*,s}$ respectively represent the effective relativistic degree of freedom that contribute to the radiation energy and entropy density, the superscript 0 denotes the present time. To determine $\Omega_{\text{GW}}(f)$, we set the values $\Omega_r/g_*^0 \approx 2.72 \times 10^{-5}$, $g_{*,s}^0 \approx 3.93$, and the functions $g_*(f)$ and $g_{*,s}(f)$ given in Ref. [71].

The priors adopted in this work are listed in Table I. By definition, the peak value P_{Rp} should not exceed $\mathcal{O}(1)$ so that R_k remains at the level of perturbations. There is no prior information for f_p since the USR regime can occur at any period during inflation. Therefore, we set f_p to be roughly within the sensitivity band of NANOGrav. The energy spectrum in our model is a convex upward curve. If f_p is below the band of NANOGrav, the spectrum can not fit the data. But if f_p is beyond the band of NANOGrav, our model can still fit the data well. So we set the upper bound of the prior for f_p two orders of magnitude higher than the band of NANOGrav. For the parameter β , theoretically it can span a large range, so we set the prior of β between 0 and 5 to study its behavior.

Results. We use the SGWB energy spectrum from USR model to fit the NG15 dataset and obtain the constraints on the model parameters. Fig. 1 shows the posterior distributions for the three model parameters. The red and blue contours denote the regions favored by the data at 68% and 95% confidence level, respectively.

TABLE I. Priors on the Model Parameters. From a physical perspective, P_{Rp} is constrained to be less than $\mathcal{O}(1)$. However, we relax this constraint to better observe the trend of $\log_{10} P_{\text{Rp}} - \log_{10} f_p$.

Parameters	Priors
P_{Rp}	Log-Uniform(-3, 1)
f_p [Hz]	Log-Uniform(-10, -5)
α	4
β	Uniform(0, 5)
γ	2.6
A_a	Log-Uniform(-20, -11)
γ_a	Uniform(0, 7)

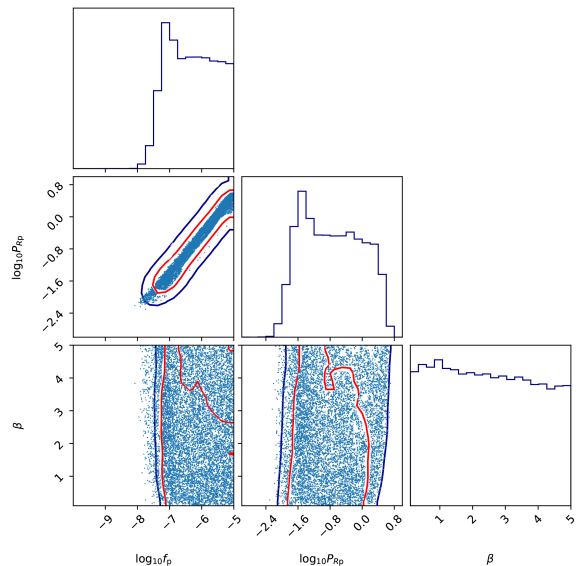


FIG. 1. Posterior distribution of three input parameters. The red and blue lines denote the 68% and 95% confidence regions, respectively.

As the PTA data points are roughly monotonically increasing, in the posterior plot, the peak of Ω_{GW} will degenerate with f_p . And the peak of $\log_{10} \Omega_{\text{GW}}$ is proportional to $\log_{10} P_{\text{Rp}}$, so we find that in the $\log_{10} P_{\text{Rp}} - \log_{10} f_p$ plot, the two parameters degenerate with each other. The degeneracy could also be found in the power-law energy spectrum model. The lower limit of $\log_{10} P_{\text{Rp}}$ is approximately -1.80 at 95% confidence level. In the one-dimensional marginalized distribution, the peak values of $\log_{10} P_{\text{Rp}}$ and $\log_{10} f_p$ are -1.69 and -6.85 , respectively. We have checked that the difference of chi-square between the peak and plateau (the flat region to the right of the peak) is about $0 \sim 4$. Besides, the parameter β is poorly constrained as expected.

In Fig. 2, we present the typical SGWB energy spectrum in our model and the data from NANOGrav dataset [5]. The red line represents the best fitting model.

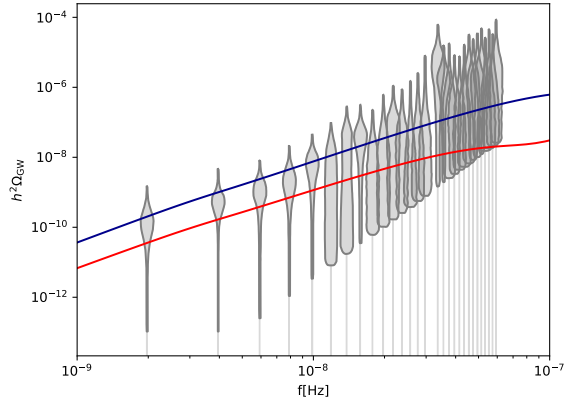


FIG. 2. The red curve represents the best fitting SGWB energy spectrum in our model, specifically with $\beta = 3$ and the other two parameters set at their peak values in the posterior. The blue curve corresponds to the SGWB spectrum with $\beta = 3$ and the other two parameters chosen from the plateau of the posterior. The gray violins are the periodogram for the free spectral process from NANOGrav dataset [5].

For comparison, we also plot the case in which parameters deviate from the peak values in the blue line. The energy spectrum in our model is a convex upward curve. So to fit the data, f_p should be at or above the NANOGrav band. The infrared spectrum of our model is governed by the spectrum index α which is a constant in our model. The UV spectrum of our model is governed by the index β . The constraining power of NANOGrav data mostly comes from the low frequency and intermediate frequency data points, so β is loosely constrained. Notably, a simple power-law model could not fit the NG15 dataset very well. The data seems to favor a steeper slope at low frequencies and a flatter slope at high frequencies. Note that the blue and red lines shown in Fig. 2 are both the infrared spectrum, i.e., the peak values are both above 10^{-7}Hz .

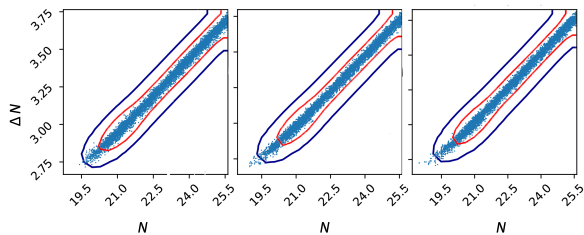


FIG. 3. The confidence contours of $N - \Delta N$ with β set as 0.5, 1 and 2 from left to right.

In Fig. 3, we present our constraints on N and ΔN , the intrinsic parameters of the USR inflation, where N and ΔN respectively denotes the e -folding number of the

end and the duration of the USR regime¹. Through an analytical calculation to predict $P_R(k)$ within the USR inflation framework, we discern the amplification rate of $P_R(k)$ at its peak to be $e^{6\Delta N}$.

To investigate the impact of β on the constraints, we choose three typical values 0.5, 1, 2 for β . The posterior distributions indicate that ΔN strongly degenerates with N . As mentioned before, β has little effect on the constraints.

Conclusions and discussions. In this work, we explore the possibility of using USR inflation to explain the NG15 dataset and obtain the favored physical parameter space of the USR regime by the data. The posterior distributions indicate strong degeneracy between $\log_{10} P_{\text{Rp}} - \log_{10} f_p$ and $N - \Delta N$. We obtain the 95% C.L. lower limit $\Delta N > 2.8$ for $N \approx 20$, regardless of the value of β . In our previous work [72], the upper limit of ΔN given by the LIGO-Virgo O3 dataset is about 2.87 for $N \approx 41.5$ with $\beta = 1$. Compared to the LIGO-Virgo data, the NG15 data place strong constraints on ΔN .

For the power spectrum of curvature perturbations, we place the limit $\log_{10} P_{\text{Rp}} > -1.80$ at 95% C.L.. Moreover, the one-dimensional posteriors of $\log_{10} P_{\text{Rp}}$ and $\log_{10} f_p$ show the presence of peaks in the NANOGrav sensitivity band. The peaks can also be found in the SIGW-Gauss model in [22] when Δ is small.

In NANOGrav's paper [22], to quantify the goodness of fit, the Bayes factors are calculated and compared among different models. However, it is quite uncertain to choose the priors for the parameters in USR inflation. The prior can span many orders of magnitude. So instead of calculating the Bayes factors, we calculate the maximum values of the log-likelihood, which are -61.9 , -63.2 , and -65.9 for USR inflation, bubble collision during the phase transition, and SMBHBs, respectively. According to the maximum log-likelihood, our model can explain the NANOGrav data better than the fiducial SMBHBs model and the bubble collision model. However, as pointed out in [22], the result strongly depends on the modeling of SMBHB population.

In Ref. [22], three SIGW models, mathematically modeled by different power spectrum $P_R(k)$ are investigated. The contours of $\log_{10} A - \log_{10} f_*$ in [22] are quite similar with $\log_{10} P_{\text{Rp}} - \log_{10} f_p$ in this work. The reason for this is that the parameters in our model are similar to that of the SIGW models in [22], such as the infrared index, the peak amplitude and the peak frequency. However, note that the energy spectrum in this work is directly calculated from USR inflation. Also as shown in the red line in Fig. 2, it has more structures than mathematically modeled spectrum.

¹The exact definition of N is $N \equiv \ln[a(t_e)/a(t_i)]$, where a is the scale factor, t_i is the time when the Hubble scale at present leaves the horizon during inflation, and t_e is the end of the USR regime.

We also provide the analysis of SIGWs from another type of $P_R(k)$ which is induced by various GW sources after inflation [73–76] and has a characteristic k^3 slope at the infrared side because of causality. At the ultraviolet side, we set a cutoff at the scale where the central-limit theorem becomes invalid. The posterior distribution is shown in Fig. 4, which is quite similar to Fig. 1, since the precision of current data is not high enough to distinguish the slope k^3 and k^4 . The result with k^3 slope agrees well with the previous one with large β since this cutoff model can be treated as an extreme USR model.

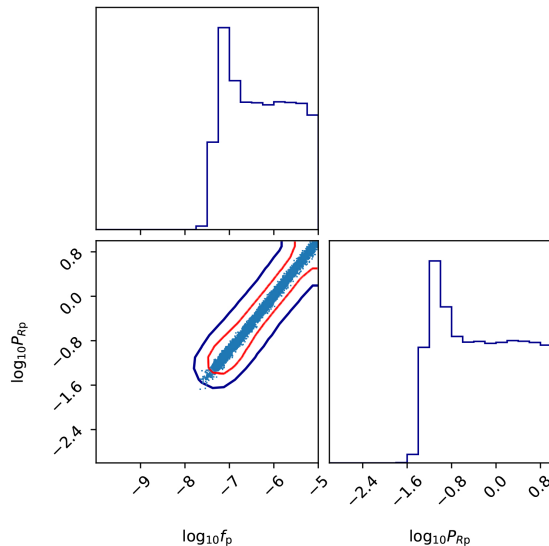


FIG. 4. Posterior distribution of the parameters in the cutoff induced SIGW. The red and blue lines denote the 68% and 95% confidence regions, respectively.

Acknowledgments This work is supported in part by the National Key Research and Development Program of China Grant No. 2020YFC2201501 and No. 2020YFC2201502, in part by the National Natural Science Foundation of China under Grant No. 12075297, No. 12235019 and No. 12105060.

* mubo22@mails.ucas.ac.cn

† liujing@ucas.ac.cn

‡ chengong@ucas.ac.cn

§ guozk@itp.ac.cn

- [1] B. P. Abbott et al., Physical Review Letters **116**, 061102 (2016).
- [2] R.-G. Cai, Z. Cao, Z.-K. Guo, S.-J. Wang, and T. Yang, Natl. Sci. Rev. **4**, 687 (2017), 1703.00187.
- [3] L. Bian et al., Sci. China Phys. Mech. Astron. **64**, 120401 (2021), 2106.10235.
- [4] H. Xu et al., Res. Astron. Astrophys. **23**, 075024 (2023), 2306.16216.

- [5] A. Afzal et al. (NANOGrav), Astrophys. J. Lett. **951** (2023), 2306.16219.
- [6] D. J. Reardon et al., Astrophys. J. Lett. **951** (2023), 2306.16215.
- [7] J. Antoniadis et al. (2023), 2306.16214.
- [8] G. Agazie et al. (2023), arXiv:2306.16213.
- [9] G. Agazie et al. (NANOGrav), Astrophys. J. Lett. **952**, L37 (2023), 2306.16220.
- [10] C. Han, K.-P. Xie, J. M. Yang, and M. Zhang (2023), 2306.16966.
- [11] S. Jiang, A. Yang, J. Ma, and F. P. Huang (2023), 2306.17827.
- [12] K. Fujikura, S. Girmohanta, Y. Nakai, and M. Suzuki, Phys. Lett. B **846**, 138203 (2023), 2306.17086.
- [13] J. Ellis, M. Lewicki, C. Lin, and V. Vaskonen (2023), 2306.17147.
- [14] Z. Wang, L. Lei, H. Jiao, L. Feng, and Y.-Z. Fan (2023), 2306.17150.
- [15] G. Lazarides, R. Maji, and Q. Shafi (2023), 2306.17788.
- [16] N. Kitajima, J. Lee, K. Murai, F. Takahashi, and W. Yin (2023), 2306.17146.
- [17] Y. Gouttenoire and E. Vitagliano (2023), 2306.17841.
- [18] L. Liu, Z.-C. Chen, and Q.-G. Huang (2023), 2307.01102.
- [19] Z.-Q. You, Z. Yi, and Y. Wu (2023), 2307.04419.
- [20] S. Wang, Z.-C. Zhao, J.-P. Li, and Q.-H. Zhu (2023), 2307.00572.
- [21] Z.-C. Zhao, Q.-H. Zhu, S. Wang, and X. Zhang (2023), 2307.13574.
- [22] A. Afzal et al. (2023), arXiv:2306.16219.
- [23] J. Liu, Z.-K. Guo, and R.-G. Cai, Phys. Rev. D **101**, 083535 (2020), 2003.02075.
- [24] O. Özsoy and G. Tasinato, JCAP **04**, 048 (2020), 1912.01061.
- [25] C. T. Byrnes, P. S. Cole, and S. P. Patil, JCAP **06**, 028 (2019), 1811.11158.
- [26] S. Pi and J. Wang (2022), 2209.14183.
- [27] J. Lin, Q. Gao, Y. Gong, Y. Lu, C. Zhang, and F. Zhang, Phys. Rev. D **101**, 103515 (2020), 2001.05909.
- [28] Z. Yi (2022), 2206.01039.
- [29] M. Cicoli, V. A. Diaz, and F. G. Pedro, JCAP **06**, 034 (2018), 1803.02837.
- [30] M. Cicoli, F. G. Pedro, and N. Pedron, JCAP **08**, 030 (2022), 2203.00021.
- [31] O. Özsoy, S. Parameswaran, G. Tasinato, and I. Zavala, JCAP **07**, 005 (2018), 1803.07626.
- [32] I. Dalianis, A. Kehagias, and G. Tringas, JCAP **01**, 037 (2019), 1805.09483.
- [33] T.-J. Gao and Z.-K. Guo, Phys. Rev. D **98**, 063526 (2018), 1806.09320.
- [34] L. Wu, Y. Gong, and T. Li, Phys. Rev. D **104**, 123544 (2021), 2105.07694.
- [35] S. S. Mishra and V. Sahni, JCAP **04**, 007 (2020), 1911.00057.
- [36] O. Özsoy and Z. Lalak, JCAP **01**, 040 (2021), 2008.07549.
- [37] B.-M. Gu, F.-W. Shu, K. Yang, and Y.-P. Zhang (2022), 2207.09968.
- [38] S. Choudhury and A. Mazumdar, Phys. Lett. B **733**, 270 (2014), 1307.5119.
- [39] C. Germani and T. Prokopec, Phys. Dark Univ. **18**, 6 (2017), 1706.04226.
- [40] N. Bhaumik and R. K. Jain, JCAP **01**, 037 (2020), 1907.04125.

- [41] K. Kefala, G. P. Kodaxis, I. D. Stamou, and N. Tetradis, *Phys. Rev. D* **104**, 023506 (2021), 2010.12483.
- [42] K. Inomata, E. McDonough, and W. Hu, *Phys. Rev. D* **104**, 123553 (2021), 2104.03972.
- [43] Y.-F. Cai, X.-H. Ma, M. Sasaki, D.-G. Wang, and Z. Zhou, *Phys. Lett. B* **834**, 137461 (2022), 2112.13836.
- [44] K. Inomata, E. McDonough, and W. Hu, *JCAP* **02**, 031 (2022), 2110.14641.
- [45] B. Carr, F. Kuhnel, and M. Sandstad, *Phys. Rev. D* **94**, 083504 (2016), 1607.06077.
- [46] S. Bird, I. Cholis, J. B. Muñoz, Y. Ali-Haïmoud, M. Kamionkowski, E. D. Kovetz, A. Raccanelli, and A. G. Riess, *Phys. Rev. Lett.* **116**, 201301 (2016), 1603.00464.
- [47] H. Di and Y. Gong, *JCAP* **07**, 007 (2018), 1707.09578.
- [48] J. Garcia-Bellido and E. Ruiz Morales, *Phys. Dark Univ.* **18**, 47 (2017), 1702.03901.
- [49] M. P. Hertzberg and M. Yamada, *Phys. Rev. D* **97**, 083509 (2018), 1712.09750.
- [50] S. Passaglia, W. Hu, and H. Motohashi, *Phys. Rev. D* **99**, 043536 (2019), 1812.08243.
- [51] R.-g. Cai, S. Pi, and M. Sasaki, *Phys. Rev. Lett.* **122**, 201101 (2019), 1810.11000.
- [52] C. Fu, P. Wu, and H. Yu, *Phys. Rev. D* **102**, 043527 (2020), 2006.03768.
- [53] Y.-F. Cai, X.-H. Ma, M. Sasaki, D.-G. Wang, and Z. Zhou (2022), 2207.11910.
- [54] D. G. Figueroa, S. Raatikainen, S. Rasanen, and E. Tomberg, *JCAP* **05**, 027 (2022), 2111.07437.
- [55] D. G. Figueroa, S. Raatikainen, S. Rasanen, and E. Tomberg, *Phys. Rev. Lett.* **127**, 101302 (2021), 2012.06551.
- [56] S. Pi and M. Sasaki (2021), 2112.12680.
- [57] Q. Wang, Y.-C. Liu, B.-Y. Su, and N. Li, *Phys. Rev. D* **104**, 083546 (2021), 2111.10028.
- [58] W.-T. Xu, J. Liu, T.-J. Gao, and Z.-K. Guo, *Phys. Rev. D* **101**, 023505 (2020), 1907.05213.
- [59] D. Y. Cheong, S. M. Lee, and S. C. Park, *JCAP* **01**, 032 (2021), 1912.12032.
- [60] M. Braglia, D. K. Hazra, F. Finelli, G. F. Smoot, L. Sri-ramkumar, and A. A. Starobinsky, *JCAP* **08**, 001 (2020), 2005.02895.
- [61] N. Aghanim et al. (Planck), *Astron. Astrophys.* **641**, A6 (2020), [Erratum: *Astron. Astrophys.* 652, C4 (2021)], 1807.06209.
- [62] R. Emami and G. Smoot, *JCAP* **01**, 007 (2018), 1705.09924.
- [63] A. D. Gow, C. T. Byrnes, P. S. Cole, and S. Young, *JCAP* **02**, 002 (2021), 2008.03289.
- [64] C. Pattison, V. Vennin, H. Assadullahi, and D. Wands, *JCAP* **08**, 048 (2018), 1806.09553.
- [65] W. G. Lamb, S. R. Taylor, and R. van Haasteren, *The need for speed: Rapid refitting techniques for bayesian spectral characterization of the gravitational wave background using ptas* (2023), 2303.15442.
- [66] J. A. Ellis, M. Vallisneri, S. R. Taylor, and P. T. Baker, *Enterprise: Enhanced numerical toolbox enabling a robust pulsar inference suite*, Zenodo (2020), URL <https://doi.org/10.5281/zenodo.4059815>.
- [67] M. Vallisneri, S. R. Taylor, J. Simon, et al., *The Astrophysical Journal* **893**, 112 (2020), URL <https://doi.org/10.3847/2F1538-4357/2Fab7b67>.
- [68] R. W. Hellings and G. S. Downs, *ApJ* **265**, L39 (1983).
- [69] K. Kohri and T. Terada, *Phys. Rev. D* **97**, 123532 (2018), 1804.08577.
- [70] J. R. Espinosa, D. Racco, and A. Riotto, *JCAP* **09**, 012 (2018), 1804.07732.
- [71] K. Saikawa and S. Shirai, *Journal of Cosmology and Astroparticle Physics* **2020**, 011 (2020), URL <https://dx.doi.org/10.1088/1475-7516/2020/08/011>.
- [72] B. Mu, G. Cheng, J. Liu, and Z.-K. Guo, *Physical Review D* **107** (2023), URL <https://doi.org/10.1103/2Fphysrevd.107.043528>.
- [73] J. Liu, L. Bian, R.-G. Cai, Z.-K. Guo, and S.-J. Wang, *Phys. Rev. Lett.* **130**, 051001 (2023), 2208.14086.
- [74] Z.-M. Zeng, J. Liu, and Z.-K. Guo, *Phys. Rev. D* **108**, 063005 (2023), 2301.07230.
- [75] T. Papanikolaou, V. Vennin, and D. Langlois, *JCAP* **03**, 053 (2021), 2010.11573.
- [76] G. Domènech, C. Lin, and M. Sasaki, *JCAP* **04**, 062 (2021), [Erratum: *JCAP* 11, E01 (2021)], 2012.08151.